Article ID: 1007－4627(2008)03－0224－08

Primary Research on Deuteron Breakup Effects with CDCC Theory*

AN Hai-xia, CAI Chong-hai

(*Insititute of Physics, Nankai University, Tianjin* 300071, *China*)

Abstract: Based on the continuum discretized coupled channels (CDCC) theory, with the suitable initial values and boundary conditions, as well as the P3C5 algorithm to solve the coupled equations, a new code CDCCOM with higher calculation precision is written to observe the deuteron breakup effects on elastic scattering angular distributions and reaction cross sections. And the validity of this code is checked. By comparing with other theories and experimental data, it is found that the present work is valuable and applicable for large nuclei range below 200 MeV, and the code is feasible for studying the breakup effect on inelastic channels further.

Key words: CDCC theory; P3C5 algorithm; breakup effect; elastic scattering angular distribution; reaction cross section

CLC number: O571.42^{+}2 **Document Code**: A

1 Introduction

Deuteron is a weakly bound nucleus with a binding energy of only 2.225 9 MeV, and it easily breaks up into proton and neutron in nuclear collisions. Some researches show that for all the nuclei studied, the proton energy spectra show large deuteron-breakup peaks centered at approximately half of the incident deuteron energy at forward angles[1]. When the breakup yield is added to the pre-equilibrium yield, the agreement with experimental data is achieved for the proton spectra. Kalbach[2] introduce an empirical formula into pre-equilibrium process to reproduce the experimental data. And it is necessary to study this phenomenon. In order to study more microcosmically the effects of deuteron breakup on inelastic channel, such as d(A, A*) n(p) cross sections and energy spectra, a new code based on the continuum discretized coupled channels (CDCC) theory[3] and the P3C5 algorithm[4] is written for studying the deuteron breakup effects on elastic channel primarily. Furthermore, the inverse kinematics reactions with deuteron targets play an important role in investigating the properties of nuclei far from stability[5, 6], and the radioactive beam facilities can provide a powerful tool to the study of these exotic nuclei[7], and generally speaking, this work is a primary work and is meaningful.

The CDCC approach is based on three body theory, and has been successful in describing the nuclear reactions with weakly bound particle as projectile. For deuteron induced reactions, it considers the interactions among p, n and target nucleus, and two relative motions, namely, the motion of n relative to p and the motion of the centre of mass of deuteron against target nucleus. The total energy of this three body system is the sum of

* **Received date**: 29 Oct. 2007; **Revised date**: 4 Dec. 2007

* **Foundation item**: Major State Basic Research Development Program of China (973 Program)(2007CB209903)

Biography: An Hai-xia(1981－), Female(Han Nationality), Inner Mongolia, Doctor Candidate, working on nuclear reaction theory and nuclear data; E-mail: anhaixia2007@yahoo.com.cn

these two relative motions and keeps fixed in the whole reaction process. Beside the ground state of deuteron, the excited states of n-p pair with certain angular momentum and continuum linear momentum is included. The continuum model space should be truncated and discretized in real calculations, then the elastic channel and discretized continuum channels are coupled to each other and affect each other.

Because the global optical potential parameters[8] can reproduce the experimental data well in a wide nucleus and energy range, it is feasible to compare the results of the CDCC with those from the global potential parameters. In this way, the effects of the deuteron breakup process on elastic scattering angular distributions and reaction cross sections are more systematically studied for many target nuclei in a wide energy region. The precision of the present calculation method is higher than that of Chau Huu-Tai[9]. By comparing the reaction cross sections and elastic scattering angular distributions derived from this work, Chau Huu-Tai's work, global potential theory with experimental values, we find that our results are reasonable, and by checking the convergence of elastic S-matrix elements, we conclude that our code is credible for further study of the breakup effects on inelastic channels.

2 Theoretical Formalism and Calculation Method

2.1 CDCC theory

By neglecting the spin of proton, neutron, target nucleus and the excitation of target, the Hamiltonian of the (A+p+n) system can be described as:

$$H(\boldsymbol{R}, E_{\mathrm{d}}) = K_{\boldsymbol{R}} + K_{\boldsymbol{r}} + U_{\mathrm{pA}}\left(\boldsymbol{r}_{\mathrm{pA}}, \frac{E_{\mathrm{d}}}{2}\right) + U_{\mathrm{nA}}\left(\boldsymbol{r}_{\mathrm{nA}}, \frac{E_{\mathrm{d}}}{2}\right) + U^{\mathrm{coul}}(\boldsymbol{r}_{\mathrm{pA}}) + V_{\mathrm{pn}}(\boldsymbol{r}) , \quad (1)$$

where $\boldsymbol{R}=(\boldsymbol{r}_{\mathrm{pA}}+\boldsymbol{r}_{\mathrm{nA}})/2$, $\boldsymbol{r}=\boldsymbol{r}_{\mathrm{pA}}-\boldsymbol{r}_{\mathrm{nA}}$, and Fig. 1 shows the relative position of this (A+p+n) system.

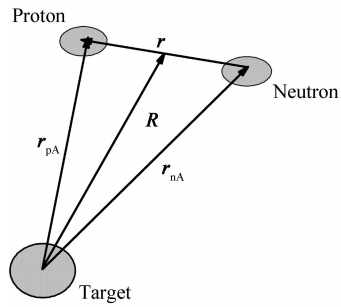

Fig. 1 The relative position coordinates of the (A+p+n) system.

The operators $K_{\boldsymbol{R}}$ and $K_{\boldsymbol{r}}$ are the kinetic energies associated with R and r. U_{nA} and U_{pA} are the nucleon-target optical potentials, and are chosen as Koning-Delaroche[10] (the corresponding spin-orbit potential is not included). $U^{\mathrm{coul}}(\boldsymbol{r}_{\mathrm{pA}})$ is the Coulomb potential of proton in deuteron relative to target nucleus. $V_{\mathrm{pn}}(\boldsymbol{r})$ is the interaction between p and n, and is chosen as a Gaussian form. This system satisfies energy conservation:

$$E_{\mathrm{d}} = \frac{\hbar^2 P_0^2}{2\mu_R} + \varepsilon_0 = \frac{\hbar^2 P_k^2}{2\mu_R} + \varepsilon_k ,$$
$$\varepsilon_k = \frac{\hbar^2 k^2}{2\mu_r} , \quad (2)$$

where ε_0 and ε_k are the eigenvalues belong to deuteron ground state and p-n continuum state with linear momentum $\hbar k$, $\hbar P_0$ and $\hbar P_k$ are the linear momentum of center of mass of p-n pair moving against target nucleus in elastic and continuum breakup channels, respectively. If J denotes the total angular momentum, L expresses the orbital angular momentum of the p-n c. m. moving against target nucleus, l represents orbital angular momentum of the p relative to n, they satisfy the sum rule $\Delta(JLl)$. In the CDCC theory, the model space needs to be truncated and discretized, the sum over l is truncated as $l \leqslant l_{\max}$; the k integral as $k \leqslant k_{\max}$; and setting the asymptotic outgoing wave boundary condition at $R=R_{\max}$. With i denotes a discretized k region Δ_i, we define $\gamma=(i, J, l, L)$ stands for the coupled channel number with the order i, J, l, L.

The coupled channels equations can be written as:

$$\left[\frac{\mathrm{d}^2}{\mathrm{d}R^2}+P_r^2-\frac{L(L+1)}{R^2}+\frac{2\mu_R}{\hbar^2}V_{\gamma\gamma}(R)\right]\times$$

$$\chi_\gamma(p_\gamma,R)=\sum_{\gamma'\neq\gamma}\frac{2\mu_R}{\hbar^2}V_{\gamma\gamma'}(R)\chi_{\gamma'}(P_{\gamma'},R)\ ,(3)$$

where χ_γ is the radial wave function for the γ-th channel, the matrix elements of coupling potentials $V_{\gamma\gamma'}(R)$ are obtained by:

$$V_{\gamma\gamma'}(R)=\langle\phi_\gamma\mid U_{\mathrm{nA}}+U_{\mathrm{pA}}\mid\phi_{\gamma'}\rangle\ , \qquad (4)$$

where ϕ_γ is the p-n pair radial wave function. The coupled channel Equations (3) are solved from $R_0=0$ to $R_{\max}$ with step ΔR, and $\chi_\gamma(P_\gamma,R)$ should satisfy the following boundary condition at $R=R_{\max}$.

$$\chi_\gamma(P_\gamma,R)\rightarrow\delta_{\gamma\gamma_0}[G_\gamma(P_\gamma,R)-\mathrm{i}F_\gamma(P_\gamma,R)]-$$

$$\sqrt{\frac{P_{\gamma_0}}{P_\gamma}}S_{\gamma,\gamma_0}[G_\gamma(P_\gamma,R)+\mathrm{i}F_\gamma(P_\gamma,R)]\ . \qquad (5)$$

The elastic S-matrix elements are used to derive the differential elastic cross section:

$$\frac{\mathrm{d}\sigma}{\mathrm{d}\Omega}=\mid f_c(\theta)+\frac{1}{2\mathrm{i}P_0}\sum_J(2J+1)\times$$

$$\mathrm{e}^{2\mathrm{i}\sigma_J}(S^J_{\gamma,\gamma_0}-1)P_J(\cos\theta)\mid^2. \qquad (6)$$

The reaction cross section can be written as:

$$\sigma_R=\frac{\pi}{P_0^2}\sum_J(2J+1)(1-\mid S^{(J)}_{\gamma,\gamma_0}\mid^2)\ . \qquad (7)$$

The partial breakup cross section is calculated with:

$$\sigma^{(J)}_{\mathrm{b},l}=\frac{\pi(2J+1)}{P_0^2}\sum_{L=|J-l|}^{J+l}\sum_{i=1}^{Nk}\mid S^{(J)}_{\gamma,\gamma_0}(k_i)\mid^2. \qquad (8)$$

2.2 Calculation method and initial values

2.2.1 P3C5 algorithm

For solving the coupled channel equations, there are mainly the following algorithms: Stormer (1907), Numerov[11], P6 and P3C5 by Clarke[4], B-splines[12]. The Numerov algorithm has a disadvantage of requiring a full matrix inversion, and it needs a long calculation time. By comparing the algorithms of Stormer, P6 and P3C5, Charke[4] proved that the P3C5 algorithm offers solutions of the highest accuracy especially with larger step lengths. Furthermore, if h denotes the step length, the error of the P3C5 is of $O(h^6)$, Stormer is of $O(h^4)$, and the spline function method adopted in Ref. [9] is of $O(h^3)$. The P3C5 algorithm requires twice as much the matrix multiplications per step and no matrix inversion is needed in the calculation process. The P3C5 algorithm is used in our code for solving the coupled channel equations. The coupled equations can be written briefly in the following form:

$$\frac{\mathrm{d}^2}{\mathrm{d}R^2}y_i(k,R)=\sum_j V_{ij}(k,R)y_i(k,R)\ , \qquad (9)$$

where y_i is the wave function for equation i ($i=1-N_{\mathrm{C}}$ and N_{C} is the number of coupled equations). The value of R from 0 to $R_{\max}$ is divided into N steps with the effective step $h=\Delta R$, and $R=n\Delta R$. V_{ij} is the effective coupling potential. In the following, we omit the index i, and let $y_n^{(2)}=h^2(\mathrm{d}/\mathrm{d}R)^2y(R)$. The P3C5 algorithm is started with the P1C3 predictor-corrector algorithm and the initial value of y_0 and y_1, four steps are made using the P1 predictor:

$$y^p_{n+1}=2y_n-y_{n-1}+y_n^{(2)}\ , \qquad (10)$$

at each step the predicted values y^p_{n+1} are substituted into Eq. (9) to yield the quantities: $y^{p(2)}_{n+1}$. The C3 corrector is used to obtain a corrected value for y_{n+1}:

$$y_{n+1}=y^p_{n+1}+\frac{1}{12}(y^{p(2)}_{n+1}-2y_n^{(2)}+y_{n-1}^{(2)})\ , \qquad (11)$$

after two steps with the P1C3, we get the values of y_2, y_3, $y_2^{(2)}$ and $y_3^{(2)}$ as starting values for P3C5 algorithm. Then for $n\geqslant3$, the full P3C5 algorithm is implemented using the P3 predictor with:

$$y^p_{n+1}=2y_n-y_{n-1}+y_n^{(2)}+\frac{1}{12}\times$$

$$(y_n^{(2)}-2y_{n-1}^{(2)}+y_{n-2}^{(2)})\ , \qquad (12)$$

again y^p_{n+1} is substituted into Eq. (9) to yield $y^{p(2)}_{n+1}$ and then the C5 corrector is used:

$$y_{n+1} = 2y_{n+1}^{p} + \frac{1}{240}(19y_{n+1}^{p(2)} - 56y_{n}^{(2)} + 54y_{n-1}^{(2)} - 16y_{n-2}^{(2)} - y_{n-3}^{(2)}) . \quad (13)$$

2.2.2 Initial values

As mentioned above, in order to solve the couple equations with the P3C5 algorithm, it is necessary to give initial values at $R=0$ and $R=\Delta R$ for each inner wave function. And in this work we choose the following initial values for the inner wave functions with definition $t=\Delta R^{J+1}$:

$$\chi_{\gamma',\gamma}(P_\gamma, R=0) = 0$$
$$\chi_{\gamma',\gamma}(P_\gamma, R=\Delta R) = \begin{cases} 0, & \gamma \neq \gamma' \\ t + \mathrm{i}t, & \gamma = \gamma' \end{cases} \quad (14)$$

where i is the unit of imaginary number. The above assumptions mean that, for the initial values at $R=0$, all the wave function matrix elements are set to be zero, and in the case of $R=\Delta R$, except the diagonal elements, all the non-diagonal elements as zero. For a certain incoming channel γ_0, the inner wave functions at $R=R_{\max}$ are expressed as:

$$\chi_{\gamma_0,\gamma}(P_\gamma, R_{\max}) = \sum_{\gamma'=1}^{N_C} a_{\gamma_0,\gamma'} \chi_{\gamma',\gamma}(P_\gamma, R_{\max}) . \quad (15)$$

With the boundary condition Eq. (5), the wave functions and their first derivatives in the inner and outer region should be continuous at matching radius, and we obtain the following $2N_C$ equations at $R=R_{\max}$:

$$\sum_{\gamma'=1}^{N_C} a_{\gamma_0,\gamma'} \{\chi_{\gamma',\gamma}[G'_\gamma(P_\gamma, R) + \mathrm{i}F'_\gamma(P_\gamma, R)] - \chi'_{\gamma',\gamma}[G_\gamma(P_\gamma, R) + \mathrm{i}F_\gamma(P_\gamma, R)]\} = 2\mathrm{i}\delta_{\gamma,\gamma_0} ,$$
$$\sum_{\gamma'=1}^{N_C} a_{\gamma_0,\gamma'} \{\chi_{\gamma',\gamma}[G'_\gamma(P_\gamma, R) - \mathrm{i}F'_\gamma(P_\gamma, R)] - \chi'_{\gamma',\gamma}[G_\gamma(P_\gamma, R) - \mathrm{i}F_\gamma(P_\gamma, R)]\} = 2\mathrm{i}\sqrt{\frac{P_{\gamma_0}}{P_\gamma}} S_{\gamma,\gamma_0} , \quad (16)$$

where $\chi'_{\gamma',\gamma}$ is the first derivative to $P_\gamma R$ at $R_{\max}$. The above first N_C equations compose a linear system of equations with N_C variables $a_{\gamma_0,\gamma'}$, which can be solved for $a'_{\gamma_0,\gamma'}$, and then the S-matrix elements can be calculated from the second N_C equations. These S-matrix elements are used for further calculation of the reaction cross sections, the breakup cross sections and the elastic scattering angular distributions.

2.3 Test of the validity of the calculation method

As mentioned above, the model space truncation is generally composed of three types, namely, truncation of l, k, R. Some studies in Refs. [13—17] indicated that $k_{\max}=1.0\ \mathrm{fm}^{-1}$, $l_{\max}=2$ and $R_{\max}=30$ fm are sufficient truncations, and because of the parity conservation, the contribution from the odd partial wave disappeared. The first two truncations are tested in this work. Fig. 2 shows the partial breakup cross sections of s-wave ($\sigma_{l=0}^{(J)}$) and d-wave ($\sigma_{l=2}^{(J)}$) varying with $k_{\max}$, and from it we can find that $\sigma_{l=0}^{(J)}$ and $\sigma_{l=2}^{(J)}$ are stable at about 0.9 fm^{-1}, this means that $k_{\max}=1.0\ \mathrm{fm}^{-1}$ is sufficient.

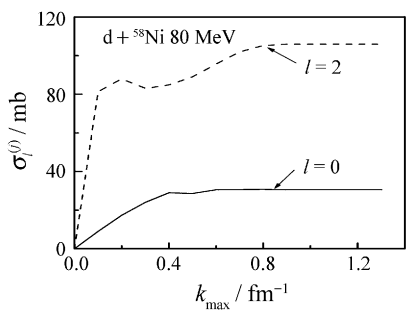

Fig. 2 The s-wave and d-wave breakup cross sections vary with increase of $k_{\max}$.

The ratios of $\sigma_{l=0}^{(J)}$, $\sigma_{l=2}^{(J)}$, $\sigma_{l=4}^{(J)}$ to the total breakup cross section σ_b are shown in Fig. 3, from it, we can see that with the $k_{\max}$ varying from 0.1 to 1.0 fm^{-1}, the $\sigma_{l=0}^{(J)}/\sigma_b$ decreases from about 0.7 to 0.2; the $\sigma_{l=2}^{(J)}/\sigma_b$, increases from about 0.2 to 0.7; at the same time, $\sigma_{l=4}^{(J)}/\sigma_b$, rises gradually, but is always lower than 0.1 and only a little larger than 0.1 for ^{58}Ni at $k_{\max}=1.0\ \mathrm{fm}^{-1}$. This means that the contributions to σ_b mainly come from $\sigma_{l=0}^{(J)}$ and $\sigma_{l=2}^{(J)}$, and the contribution of $\sigma_{l=4}^{(J)}$ can be ignored for saving computing time, $l_{\max}=2$ is enough

when $k_{max}=1.0\ fm^{-1}$.

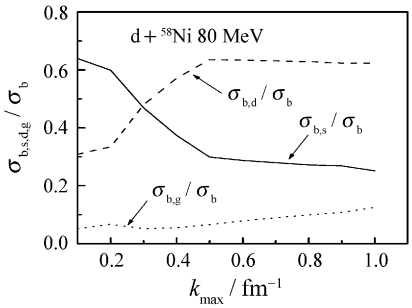

Fig. 3 With the increase of K_{max}, the ratios of s-wave, d-wave and g-wave partial breakup cross sections to the total breakup cross sections.

The elastic scattering S-matrix elements with respect to J are shown in Fig. 4, the $\mathrm{Im}S_J$ is convergent to zero and the $\mathrm{Re}S_J$ is convergent to one. These perfect convergences mean that the present calculation method is valid.

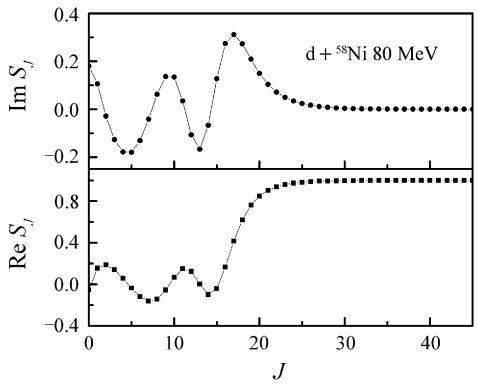

Fig. 4 The relation of real and imaginary parts of elastic S-matrix elements varying with the J.

3 Calculating Results and Discussion

The calculated elastic scattering angular distributions and the reaction cross sections of d+^{58}Ni are shown in Fig. 5 and Fig. 6, respectively.

By comparing the results of the global potential theory, this work and Chau Huu-Tai's work with experimental data, from Fig. 5 we can find that both this work and Chau Huu-Tai's work can not agree experimental data as well as the global potential theory in 30—50 degrees and the results of this work are distinctly better than those of Chau Huu-Tai's work in the angular region larger than about 50 degree. From Fig. 6 we can see that the reaction cross sections of this work keep accordance well with those of the global potential theory and the experimental values when the incident energy is lower than about 70 MeV, however, the results of Chau Huu-Tai's work are obviously larger than the experimental values. When the incident energy is larger than about 70 MeV, the results of this work and Chau Huu-Tai's work are closed to each other and lower than those of global potential theory.

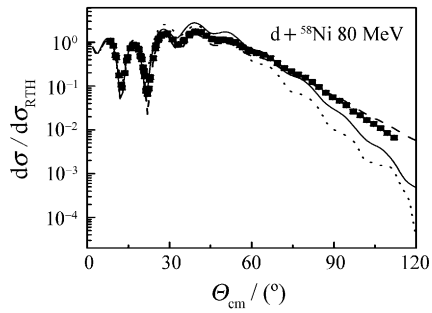

Fig. 5 For d+^{58}Ni at 80 MeV, the ratio of elastic scattering angular distributions relative to corresponding Rutherford values. The experimental data are from Ref. [18]. The results from this work, global deuteron potential and Ref. [9] are plotted with solid, dash and dot lines, respectively.

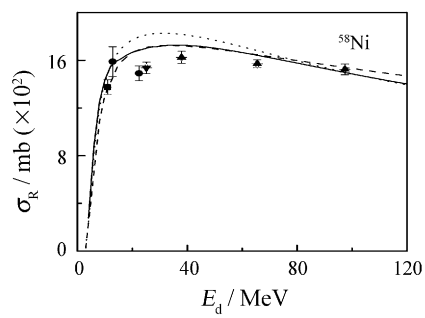

Fig. 6 Comparison of the reaction cross sections. The experimental data are from Refs. [19—22] and for more details, see the caption of Fig. 5.

For more target nuclei and widely energy range, the elastic scattering angular distributions are shown in Fig. 7 and Fig. 8. Totally speaking, the CDCC results can not fit experimental data as well as global potentials values. Comparing with

the lines of global potentials, some fluctuations appear in angular distributions at 17 MeV in Fig. 7, and this phenomenon nearly disappeared at about 170 MeV in Fig. 8. Meanwhile, with the increasing of target mass, the fluctuations become weak gradually.

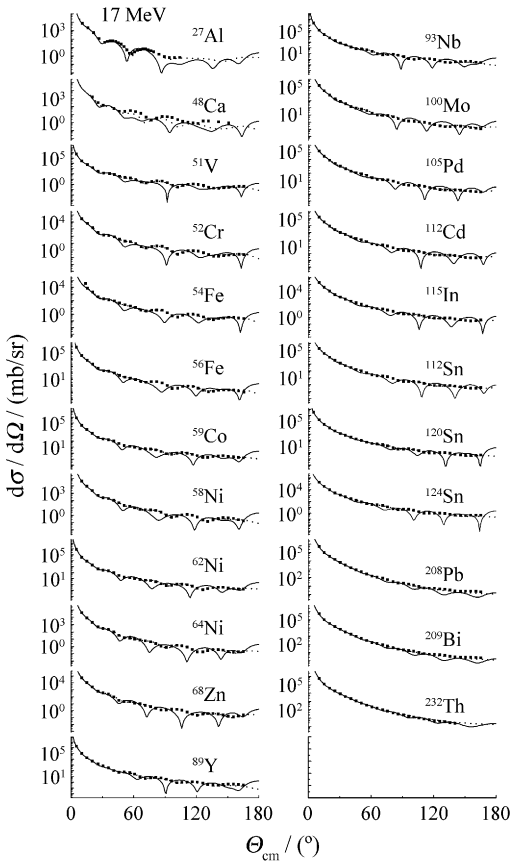

Fig. 7 The elastic scattering angular distributions for the target nuclei ranging from ^{27}Al to ^{232}Th at 17 MeV. The experimental data are from Ref. [23]. The results using this work and global potential are plotted as solid and dash lines.

In order to make clear the possible reasons, the elastic scattering angular distributions are also calculated with the folding optical model. The potential of deuteron is folded by that of neutron and proton in the Koning-Delaroche potentials (same as the nucleon-target optical potential adopted in this work). For the sake of studying the influence of the spin-orbit potential to the elastic scattering angular distribution, both with and without the spin-orbit potential the calculations are cariced out using folding model for d + ^{58}Ni at 17 MeV and the results are shown in Fig. 9. From it we can find

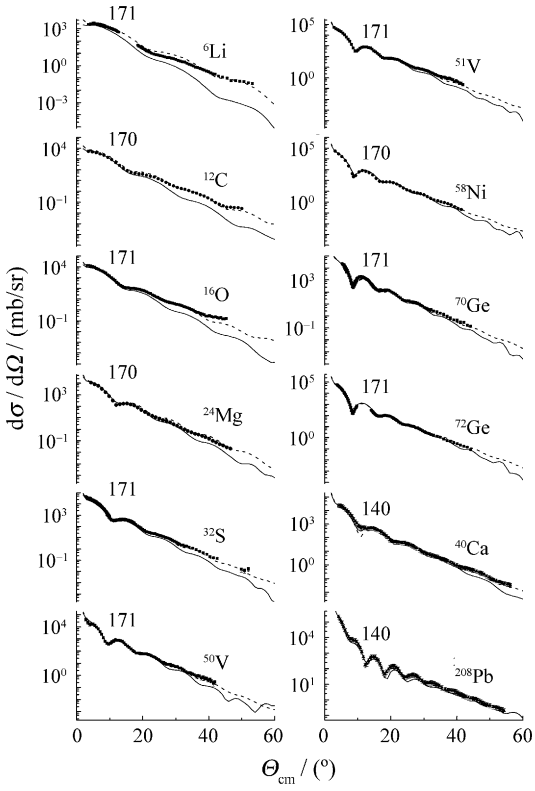

Fig. 8 The elastic scattering angular distributions at 171 and 140 MeV for the target nuclci from ^{6}Li to ^{208}Pb. The experimental data are from Refs. [24—26] and for more details, see the caption of Fig. 7.

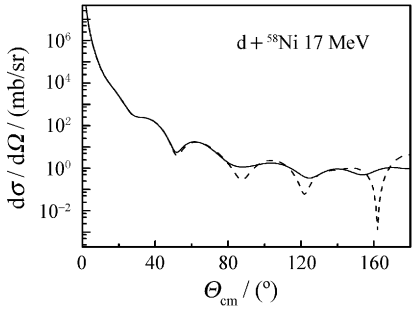

Fig. 9 Comparison of the elastic scattering angular distributions using the folding optical model with and without the spin-orbit potential plotted as solid line and dash line respectively.

that, compared with the result included spin-orbit potential, the value calculated without spin-orbit potential shows some fluctuations about larger than 40 degree, this means that the spin-orbit po-

tential affects the structure of the elastic scattering angular distributions to a certain extent. Since the spin-orbit part of nucleon-target potential is ignored and no free parameters are included in the CDCC calculations, and the break-up channels affect elastic channel by coupling more or less, the fluctuations appeared in CDCC results are acceptable, and by comparing with the experimental data, the results of CDCC are physically reasonable.

4 Summary

Based on the CDCC theory and the P3C5 algorithm with higher precision, a new code is written and checked. By comparing the reaction cross sections and elastic scattering angular distributions derived from this work, Chau Huu-Tai's work , the global potential theory with experimental values, we know that the results of this work can generally fit experimental data, and better than those of Chau Huu-Tai's work , then this code can be used for studying the effects of deuteron break-up on the inelastic channels in the future.

参考文献(References):

[1] Wu J R, Chang C C, Holmgren H D. Phys Rev, 1979, **C19**: 698.

[2] Kalbach C. Phys Rev, 2005, **C71**: 034 606.

[3] Austern N, Iseri Y, Kamimura M, *et al*. Phys Rep, 1987, **154**: 125.

[4] Clarke N M. J Phys Nucl Phys, 1984, **G10**: 1 535.

[5] Mittig W, Savajols H, Demonchy C E, *et al*. Nucl Phys, 2003, **A722**: C10.

[6] Keeley N, Alamanos N, Lapoux V. Phys Rev, 2004, **C69**: 064 604.

[7] Li Chen, Ye Yanlin, Jiang Dongxing, *et al*. Nuclear Physics Review, 2007, **24**(1): 21(in Chinese).
(李 琛, 叶沿林, 江栋兴等. 原子核物理评论, 2007, **24**(1): 21.)

[8] An Haixia, Cai Chonghai. Phys Rev, 2006, **C73**: 054 605.

[9] Chau Huu-Tai P. Nucl Phys, 2006, **A773**: 56.

[10] Koning A J, Delaroche J P. Nucl Phys, 2003, **A713**: 231.

[11] Numerov B V. Mon Not R Astron Soc, 1924, **84**: 592.

[12] Fernando Martin. J Phys, 1999, **B32**: R197.

[13] Yahiro M, Nakano M, Iseri Y, *et al*. Prog Theor Phys, 1982, **67**: 1 467.

[14] Piyadasa R A D, Kawai M, Kamimura M, *et al*. Phys Rev, 1999, **C60**: 044 611.

[15] Kamimura M, Yahiro M, Iseri Y, *et al*. Prog Theor Phys Suppl, 1986, **89**: 1.

[16] Piyadasa R A D, Yahiro M, Kamimura M, *et al*. Prog Theor Phys, 1989, **81**: 910.

[17] Yahiro M, Kamimura M. Prog Theor Phys, 1981, **65**: 2 051.

[18] Stephenson E J, Collins J C, Foster C C, *et al*. Phys Rev, 1983, **C28**: 134.

[19] Auce A, Carlson R F, Cox A J, *et al*. Phys Rev, 1996, **C53**: 2 919.

[20] Mayo S, Schimmerling W, Sametband M J, *et al*. Nucl Phys, 1965, **62**: 393.

[21] Budzanowski A, Growski K. Phys Lett, 1962, **2**: 280.

[22] Bearpark K, Graham W R, Jones G. Nucl Phys, 1965, **73**: 206.

[23] Childs J D, Daehnick W W, Spisak M J. Phys Rev, 1974, **C10**: 217.

[24] Bäumer C, Basini R, van den Berg A M, *et al*. Phys Rev, 2001, **C63**: 037 601.

[25] Korff A, Haefner P, Bäumer C, *et al*. Phys Rev, 2004, **C70**: 067 601.

[26] Okamura H, Ishida S, Sakamoto N, *et al*. Phys Rev, 1998, **C58**: (4): 2 180.

基于 CDCC 理论对氘核破裂效应进行初步研究*

安海霞[1)]，蔡崇海

（南开大学物理科学学院，天津 300071）

摘　要：为研究氘核的破裂效应对弹性散射角分布和反应截面的影响，基于连续离散化耦合道（CDCC）理论编制了程序 CDCCOM。从中心点波函数的初始值出发，利用 P3C5 算法求解耦合道方程组，进而通过边界点上内、外区的波函数相匹配求得 S 矩阵元。P3C5 算法提高了计算精度，同时验证了程序 CDCCOM 的有效性。通过与其他工作的计算结果及实验数据进行比较，认为在氘核入射能量低于 200 MeV 的情况下，对于大多数靶核，通过 CDCCOM 都能够得出合理的结果，表明该程序可用于进一步研究氘核诱发的非弹性核反应。

关 键 词：CDCC 理论；P3C5 算法；破裂效应；弹性散射角分布；反应截面

*　**收稿日期**：2007-10-29；**修改日期**：2007-12-04

*　**基金项目**：国家重点基础研究发展计划（973 计划）资助项目（2007CB209903）

1)　E-mail：anhaixia2007@yahoo.com.cn